Electronic state characterization of SiO$_x$ thin films prepared by evaporation

A. Barranco[a)]
*Nanotech@surfaces Laboratory, Materials Science and Technology (Empa), Feuerwerkerstrasse 39,
CH-3600 Thun, Switzerland and Physics Department, University of Fribourg, Pérolles, CH-1700 Fribourg,
Switzerland*

F. Yubero and J. P. Espinós
*Institute of Materials Science of Seville [Consejo Superior de Investigaciones Científicas (CSIC)–University
of Seville], Avenida Américo Vespucio s/n. 41092 Sevilla, Spain*

P. Groening
*Nanotech@surfaces Laboratory, Materials Science and Technology (Empa), Feuerwerkerstrasse 39,
CH-3600 Thun, Switzerland and Physics Department, University of Fribourg, Pérolles, CH-1700 Fribourg,
Switzerland*

A. R. González-Elipe
*Institute of Materials Science of Seville [Consejo Superior de Investigaciones Científicas (CSIC)–University
of Seville], Avenida Américo Vespucio s/n. 41092 Sevilla, Spain*

SiO$_x$ thin films with different stoichiometries from SiO$_{1.3}$ to SiO$_{1.8}$ have been prepared by evaporation of silicon monoxide in vacuum or under well-controlled partial pressures of oxygen ($P < 10^{-6}$ Torr). These thin films have been characterized by x-ray photoemission and x-ray-absorption spectroscopies, this latter at the Si K and $L_{2,3}$ absorption edges. It has been found that the films prepared in vacuum consists of a mixture of Si^{3+} and Si$^+$ species that progressively convert into Si^{4+} as the partial pressure of oxygen during preparation increases. From this spectroscopic analysis, information has been gained about the energy distribution of both the full and empty states of, respectively, the valence and conduction bands of SiO$_x$ as a function of the O/Si ratio. The characterization of these films by reflection electron energy-loss spectroscopy (REELS) has provided further evidences about their electronic structure (band gap and electronic states) as a function of the oxygen content. The determination of the plasmon energies by REELS has also shown that the films prepared by evaporation in vacuum consist of a single phase which is characterized by a density (1.7 g cm^{-3}) lower than that of SiO$_2$ (i.e., 2.2 g cm^{-3}) or Si (i.e., 2.4 g cm^{-3}). The optical properties (**n** and **k**) of the films as a function of the O/Si content have been deduced from the analysis of REELS spectra in the energy range from 4 to 20 eV. It has been also shown that the O/Si ratio in the films and several spectroscopic parameters such as the Auger parameter or the energy of bulk plasmons present a linear relationship and that this linear dependence can be used for a rapid characterization of SiO$_x$ materials. By contrast, the band-gap energy changes differently with the O/Si ratio, following a smooth linear increase from about 3.8 eV for SiO$_{1.3}$ to ca. 5.0 eV for SiO$_{1.7}$ and a jump up to 8.7 eV for SiO$_2$. These results indicate that the random-bonding model does not apply to thin films prepared by evaporation under our experimental conditions. Other distributions of Si^{n+} states can be induced if the films are excited with an external source such as heat or photon irradiation. In this case the electronic properties vary and the previous linear correlations as a function of the oxygen content do not hold any longer.

I. INTRODUCTION

Nonstoichiometric silicon oxides (SiO$_x$ with $x < 2$) thin films have been widely studied during the last decades due to their numerous technological applications. The interest in these films began with their use as passivation layers, dielectric films, and interlayers in microelectronics.[1,2] SiO$_x$ layers have been also used as protective coatings in metallic mirrors, antireflection coatings, or low index layers in the mid-infrared range.[3–5] SiO$_x$ thin films are also being employed for

the fabrication of light-emitting silicon-based structures.[6,7] These latter consist of silicon nanocrystals embedded in a silica matrix and are obtained by disproportionation reaction of the Si^{n+} ($0 < n < 4$) species present in the SiO$_x$. Annealing in vacuum or in an inert gas[8–10] or exposure to a laser[7,11] or an intense source of ultraviolet (UV) light[12] have been used to induce such a reaction.

Different models have been proposed to account for the distribution of Si^{n+} species in SiO$_x$ thin films.[13–15] These models were originally developed to account for the distribution of Si^{n+} states at the interface between Si and a thermally grown silicon oxide overlayer, although they have also been used to describe the distribution of Si^{n+} species in SiO$_x$

[a)]Author to whom correspondence should be addressed; FAX: +34954460665; electronic mail: angelbar@icmse.csic.es

thin films. In the mixture model (MM) SiO_x is described as a mixture of Si^0 and Si^{4+} species (i.e., $Si–Si_4$ and SiO_4 tetrahedral units).[13,15] The more widely accepted model is the so-called random-bonding model (RBM). It considers that the films are built up by several tetrahedral units $Si–O_xSi_{(4-x)}$ ($x = 0, \ldots, 4$) that follow a simple statistical distribution.[13–15] Although the structure and the electronic and optical properties of SiO_x materials have been extensively discussed within the frame of this RBM, some controversy has arisen about its general applicability. This controversy stems from experimental evidences showing that in SiO_x thin films with a given O/Si ratio, different distributions of oxidation states can be found according to the method of preparation.[12,16,17] Thus, in previous works, we have found that SiO_x thin films deposited at room temperature by evaporation of silicon monoxide do not follow the distribution of Si^{n+} states predicted by the RBM.[10,12,18] We also showed that these SiO_x films were in a metastable state and that either by light excitation[12] or ion-beam irradiation[19] the distribution of Si^{n+} species may change while keeping constant the overall O/Si ratio.

Most experimental procedures employed for the preparation of SiO_x thin films are based on chemical or physical phenomena that, directly or indirectly, may induce some kind of excitation of the growing layers. This is the case of sputtering[13] or plasma processes[16,20,21] where ion bombardment, UV-light irradiation, or the supply of thermal energy might lead to a redistribution of oxidation states in the SiO_x thin films and, therefore, to changes in their properties. Since the influence of these processes is not well controlled or even recognized, a comparison of the published results on SiO_x prepared by different procedures is not always straightforward.

As a continuation of our previous investigations on SiO_x thin films prepared by evaporation of silicon monoxide we present here a multitechnique study of their electronic properties and on how these properties change with the O/Si ratio. The analysis is done by means of surface sensitive techniques, such as x-ray photoemission spectroscopy (XPS), x-ray-absorption spectroscopy (XAS), and reflection electron energy-loss spectroscopy (REELS). A first objective of this investigation is to provide experimental correlations between the O/Si stoichiometry and electronic properties of well-characterized SiO_x thin films prepared without external excitation. A second objective is to provide reference data to evidence possible changes in the electronic properties of these materials due to alternative distributions of Si^{n+} states induced by an external excitation.

II. EXPERIMENT

Silicon oxide (SiO_x with $x < 2$) thin films were prepared by thermal evaporation of silicon monoxide brown powder (Goodfellow) with a Knudsen cell. Full details about the deposition method and experimental conditions can be found elsewhere.[12] The SiO_x thin films were deposited at room temperature on flat one-side-polished Si(100) wafers. The stoichiometry of the SiO_x films was varied by evaporation of the silicon monoxide compound in increasingly higher par-

tial pressures of oxygen from $10^{-8} < P < 10^{-6}$ Torr. In some cases the evaporated SiO_x layers were heated under ultrahigh-vacuum (UHV) conditions ($P < 10^{-8}$ Torr) at 750 K for 3 h; this treatment produces dissociation of the structure and the formation of Si^0 species. In the text, this sample rich in Si^0 will be labeled as $SiO_x[Si^0]$.

Chemical and electronic information of the topmost (~ 5 nm) surface region of the obtained thin films was studied *in situ* after deposition. The films were characterized by electron spectroscopies such as XPS, photoemission spectroscopy (PES) with synchrotron radiation, and REELS.

XPS spectra were acquired with a VG-ESCALAB 210 spectrometer. It was operated at a constant pass energy with a value of 20 eV. Unmonochromatized Mg $K\alpha$ radiation was used as excitation source. The Si $2p$ and O $1s$ photoemission peaks and the Si KLL and O KLL Auger peaks were recorded. The resolution was such that the width of the Si $2p$ of a clean silicon sample was 1.2 eV.

For the characterization by REELS, primary beam energies between 200 and 2000 eV with an energy resolution of ~ 0.7 eV were used. The measurements were done in the XPS chamber by using a VG electron source (LEG 6000). The angle of incidence was 60° with respect to the normal surface. The reflected electrons were analyzed in an angle normal to the surface. The **n** and **k** functions in an energy range from 4 to 20 eV and the absorption coefficients (α) were extracted from the REELS spectra following a procedure described in a previous paper.[22] The optical band gaps were also estimated from the REELS spectra by considering the photon energy at which $\alpha \leqslant 10^4$ cm^{-1}.[22–24]

Photoemission with synchrotron radiation (PES) was done at the KMC beam line of the BESSY synchrotron in Berlin. Si $L_{2,3}$ XAS spectra were recorded in the same line by total electron yield measurements. XAS spectra at the Si K edge were recorded at the SA32 beam line of the Super-Aco synchrotron (LURE, Orsay). An InSb(111) double-crystal monochromator was used for selection of the photon energy (resolution of 0.75 eV at 2000 eV). The spectra were recorded by measuring the drain current through the sample (total electron yield detection).

III. RESULTS AND DISCUSSION

A. Distribution of Si^{n+} species in SiO_x thin films: Stoichiometry and local structure around Si

A set of SiO_x thin films with thickness of the order of 100 nm were prepared by evaporation of silicon monoxide in the UHV chamber at increasing oxygen partial pressures between 10^{-8} and 10^{-6} Torr. The stoichiometry of the films was controlled by *in situ* XPS at several stages of the film preparation. In previous works we have reported about the distribution of Si^{n+} states in this type of films deduced by XPS, PES, extended x-ray-absorption fine structure (EXAFS),[12] x-ray-Absorption Near-Edge Spectroscopy (XANES), and resonant Auger spectroscopy.[10] Thus, it was found that the structural data obtained by EXAFS assuming the presence of Si^{3+} and Si^+ species were in agreement with the fitting analysis of Si $2p$ photoemission spectra. These results and the calculation procedures will not be discussed
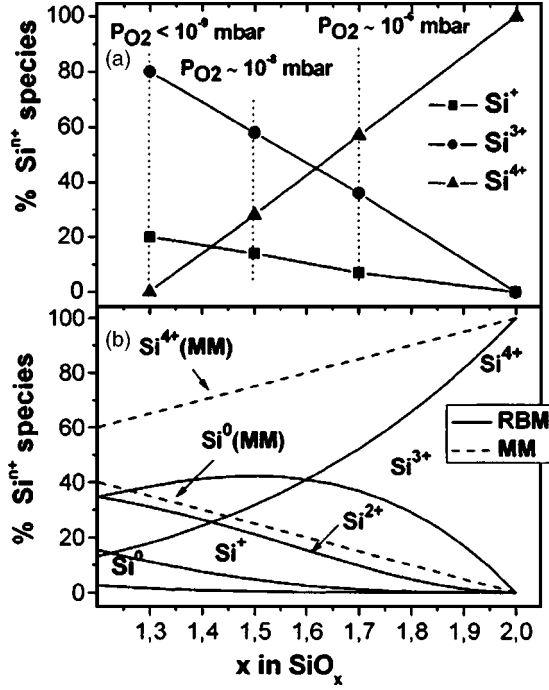
FIG. 1. (a) Distribution of Si^{n+} species as a function of the oxygen content determined experimentally for SiO_x thin films prepared by evaporation. (b) Distribution of Si^{n+} species as a function of the oxygen content predicted by the MM and RBM.

FIG. 2. Evolution of the Auger parameters of Si and O as a function of the oxygen content in SiO_x thin films prepared by evaporation.

obtain the distribution of Si^{n+} states predicted by that model.

B. Auger parameter and thin-film stoichiometry

For a given element, its Auger parameter (α') in a compound is defined as the sum of the binding energy (BE) of a photoelectron peak and the kinetic energy (KE) of an Auger peak.[25,26] This parameter can be taken as a measurement of the extra-atomic relaxation energy of photoholes and therefore depends on the electronic properties of the material hosting that element. The exact definition of α' refers to a given oxidation state of an element and therefore its application to SiO_x would imply a precise deconvolution of both the Si $2p$ photoemission and Si KLL Auger spectra. Particularly for the latter, such a deconvolution is not straightforward and, following the approach of Alfonsetti et al.,[26] we prefer to apply the Auger parameter concept to the centroids of the Si $2p$ and Si $KL_{2,3}L_{2,3}$ spectra. This definition is not subjected to ambiguities and can be directly correlated with the stoichiometry and electronic properties of SiO_x compounds. Figure 2 shows the experimental values obtained for this averaged Auger parameter as a function of the content of oxygen in the films. The plotted straight line is a linear regression to the experimental points and can be used as a phenomenological relationship to identify the stoichiometry of SiO_x compounds according to the expression

$$\alpha'(Si) = 1713.5 + 2.3(2 - x). \tag{1}$$

This linear correlation agrees quite well with that found by Alfonsetti et al.[26] for SiO_x thin films prepared by a similar preparation procedure. In the present investigation we have also carried out the evaluation of the Auger parameter for the oxygen peaks. This analysis is interesting because, contrary to the Si $2p$ and Si $KL_{2,3}L_{2,3}$ peaks that are broadened because of the superposition of the components of the different oxidation states of silicon (i.e., Si^{n+} species), the oxygen peak virtually maintains the same width irrespective of the actual O/Si ratio. This behavior can be explained by considering that in the SiO_x the oxygen atoms are always bonded as a bridge between two silicon atoms. The evolution of the Auger parameter of oxygen $[\alpha'(O)=O\ 1s\ BE+O\ KVV\ KE]$ as a function of stoichiometry is also represented in Fig. 2. The slope defined by these points and therefore the difference between the values for $SiO_{1.3}$ and SiO_2 [i.e., $\Delta\alpha'(Si)$

any longer here but will be directly used to ascertain the distribution of Si^{n+} states in our films as a function of the oxygen content. Figure 1(a) shows the percentage of the different oxidation states of silicon determined by XPS in previous publications[10,12] for films with different O/Si ratios prepared under oxygen partial pressures in the range of 10^{-9} to 10^{-6} Torr. Figure 1(b) shows the theoretical distribution of Si^{n+} species according to the MM and RBM as a function of this ratio.[13] A comparison between the two figures shows clearly that the distribution of the Si^{n+} species in our films does not follow the distribution predicted by any of the two models. For example, in the MM a film of global stoichiometry $SiO_{1.3}$ contains 35% of Si^0 and 65% of Si^{4+} species [cf. Fig. 1(b)]. Meanwhile, according to the RBM, a film of this stoichiometry would consist of a mixture of 2% Si^0, 11% Si^+, 31% Si^{2+}, 38% Si^{3+}, and 18% Si^{4+} [cf. Fig. 1(b)]. By contrast, the experimental composition determined for a film of that stoichiometry is 23% Si^+ and 77% Si^{3+} [cf. Fig. 1(a)]. The most outstanding result from these experiments is the practical absence of Si^0 and Si^{2+} species in all the layers.[10,12] The particular distribution of species in these films was discussed in terms of kinetic constraints that hinder the disproportionation of Si^{3+} and Si^+ into Si^0 and Si^{4+} species.[12] Meanwhile, it was shown that the disproportionation of Si^{2+} species into Si^+ and Si^{3+} species is a reaction thermodynamically favored and with a relatively low-energy activation barrier, two features that explain the absence of the Si^{2+} species in our films.[12] The existence of activation barriers and kinetic constraints in SiO_x thin films grown at room temperature contradicts the basic assumption of the RBM (i.e., equal probability for the different types of fourfold-coordinated Si atoms) and explains why we do not
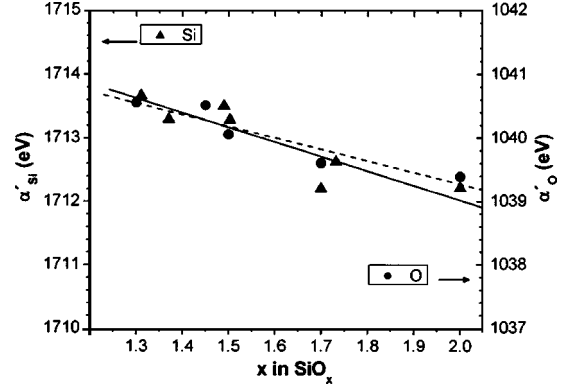
~ 1.4 and $\Delta\alpha'(O) \sim 1.2$ eV] are quite similar, likely indicating that for the two atoms the relaxation processes depend on similar physical variables. In contrast with the similar evolution with x of $\alpha'(Si)$ and $\alpha'(O)$, BEs of Si $2p$ and O $1s$ peaks present a different behavior. Thus, while the centroid of the Si $2p$ peak shifts by ~ 1.3 eV from $SiO_{1.3}$ to SiO_2 (note that the BE difference between Si^0 and Si^{4+} species in, respectively, metallic silicon and SiO_2 is ~ 4 eV),[27] the O $1s$ peak remains practically constant at a fixed BE of 532.6 eV.

Differences in the Auger parameter ($\Delta\alpha$) are related to differences in the extra-atomic relaxation energies (REs) in the final state by the expression[25]

$$\Delta\alpha = 2\Delta RE. \qquad (2)$$

Meanwhile, the difference in BEs accounts for differences in both the initial (ε) and final-state energies according to[25]

$$\Delta BE = \Delta\varepsilon + \Delta RE. \qquad (3)$$

For the analyzed samples the maximum differences in the value of the different energetic terms estimated through (2) and (3) are as follows: $\Delta RE(Si) = 0.7$ eV, $\Delta RE(O) = 0.6$ eV, $\Delta\varepsilon(Si) = -0.1$ eV, $\Delta\varepsilon(O) = -0.6$ eV. The similar values of ΔRE determined for both silicon and oxygen indicate that the medium surrounding the two atoms relaxes similarly upon the creation of a photohole. This similarity supports that our samples are homogeneous and consist of a single phase. The higher value of RE obtained for the $SiO_{1.3}$ samples must be related to the higher electron density determined by plasmon analysis (see below in Sec. III E). By contrast, ε changes by -0.6 eV when determined for the oxygen and only by -0.1 eV when estimated for the silicon. According to (3), this means that for oxygen $\Delta\varepsilon$ must compensate ΔRE almost exactly. Changes in ε occur because of differences in the density of charge at the oxygen atom or in the value of the Madelung potential around it. Oxygen atoms in SiO_x are bridging between two Si^{n+} ions whose actual densities of charge will depend on their formal charge n. As n increases (i.e., towards Si^{4+}) the positive Madelung potential due to the neighboring silicon ions increases. We attribute the decrease of -0.6 eV in $\varepsilon(O)$ measured for $SiO_{1.3}$ with respect to SiO_2 to a larger Madelung potential and an increasingly higher density of negative charge at the oxygen sites for samples with the SiO_2 stoichiometry. Similarly, intermediate deviations are expected for samples with $1.3 < x < 2$.

C. Valence-band states: XPS versus PES

The occupied states of the valence band of SiO_x thin films were analyzed by XPS and PES. Valence-band spectra of SiO_x thin films excited with photon energies of 140 eV (PES) and 1253.6 eV (XPS) are shown in Figs. 3 and 4. The comparison of these two types of spectra permits to identify the different element and orbital contributions to the valence band. In fact, owing to the different photoexcitation cross sections for the O $2p$, Si $3p$, and Si $3s$ states that upon hybridization defined the occupied levels of the valence band of SiO_x compounds, the intensity of the different bonds of the spectra change with the photon energies used for photoexcitation.[13,28] From the comparison of these two fig-
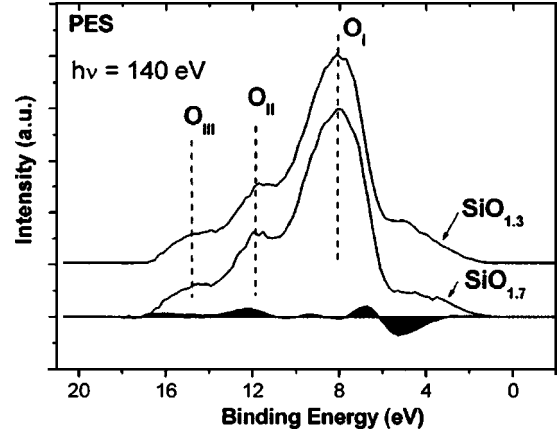

FIG. 3. PES spectra ($h\nu = 140$ eV) of two SiO_x thin films with different O/Si ratios. The shadowed curve corresponds to the difference spectra between the two plots.

ures and taking into account the cross sections, it appears that the VB states at ~ 8 eV whose intensities are enhanced in PES have a predominant O $2p$ character. Meanwhile, the structures between 10 and 17 eV whose intensities are enhanced by a factor ~ 10 by using higher photon energies in XPS must be attributed to Si $3p$ and Si $3s$ states.[28]

Along with this preliminary attribution four main structures can be identified in the spectra of Figs. 3 and 4. The feature labeled O_1 and located at ~ 7.5 eV corresponds to the O $2p$ lone pairs of the SiO_x structure.[13,14] Besides, two other features, labeled O_{II} and O_{III} and located at ~ 12 and ~ 15 eV, correspond to O $2p$ states strongly hybridized with Si $3p$ and Si $3s$ levels, respectively. The feature at ~ 4 eV corresponds to Si–Si bonding states in SiO_x.[13,14,23] The Si $3p$
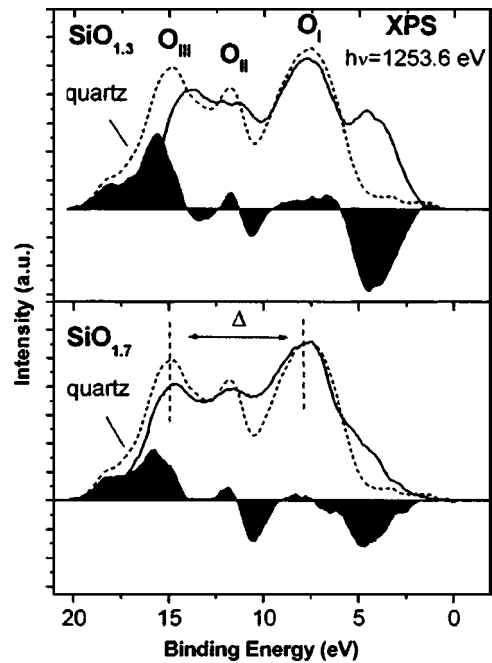

FIG. 4. XPS spectra ($h\nu = 1253.6$ eV) of two SiO_x thin films with different O/Si ratios. The dashed curve is the spectrum of a fully stoichiometric SiO_2, while the shadowed curves are the difference spectra between the spectra of SiO_x and SiO_2.

character of this latter feature is demonstrated by the enhancement of its intensity in the XPS spectra (cf. Figs. 3 and 4).[13]

Figures 3 and 4 also show a comparative analysis of the spectra of SiO_x samples with different O/Si ratios. The shadowed curves are the differences between the two spectra in each figure and represent the changes due to the formation of direct Si–Si bonds in SiO_x. These difference curves, particularly for the XPS spectra, show that the intensity of the peak at 4 eV increases as the oxygen content in the film decreases (i.e., difference curve with negative sign). A decrease in intensity is also observed in the XPS spectra at the valley around 10-eV BE. Meanwhile, for low stoichiometries, the O_{III} feature depicts a net increase in intensity and a shift in position. Similar tendencies are also found for O_{II}, although the changes are less pronounced. No noticeable changes occur for feature O_I. The separation Δ between the maximum of the O $2p$–lone pair (feature O_I) and the O$2p$–Si$3p$ states took the values of 6.0, 6.8, and 7.2 eV for $x=1.3$, 1.7, and 2.0 respectively. This shift, as well as the enhancement of the gap between the O $2p$–lone pair states and the O $2p$–Si $3p$ features, is consistent with previous results reported in literature for other SiO_x thin films.[13]

The spectra in Figs. 3 and 4 also show that the intensity of the Si $3p$ features at $\sim$4 eV decreases in intensity as x increases, although it is still important for O/Si ratios as high as 1.7. Previous results in literature for SiO_x thin films with a distribution of oxidation states following the RBM show that the intensity of Si $3p$ states abruptly vanishes for x values in the range of 1.3–1.5.[13,14,23] On the other hand, theoretical calculations by Martinez and Yndurain[14] based on this model predicts that a minimum length of $\sim$10 atoms in the Si–Si chains is necessary to observe Si–Si bonding states (i.e., Si $3p$ states) in the valence band. Taken these two assertations into account, our VB spectra provide an additional confirmation that the distribution of Si^{n+} species in our films differs from that predicted by the RBM. This is in fact supported by the presence of a noticeable peak at 4 eV in the VB spectra of films with a relatively high O/Si ratio (cf. $SiO_{1.7}$ films in Figs. 3 and 4). This high intensity supports the existence in these samples of long chains where the Si is bonded to another Si ion and contradics the predictions of that model.

D. Conduction-band states: XAS characterization of SiO$_x$

The unoccupied states of the conduction band of the SiO_x thin films have been investigated by XAS. Si $L_{2,3}$ edge and Si K spectra were recorded for several SiO_x thin-film samples. These spectra are shown in Figs. 5 and 6. According to the dipolar selection rule, Si $L_{2,3}$ and Si K spectra can be considered, respectively, as a representation of the distribution of Si $3s$, Si $3d$, and Si $3p$ states in the conduction band.

A discussion about the electronic origin of the different structures appearing in the Si $L_{2,3}$ and Si K absorption spectra of SiO_2 thin films can be found in the bibliography.[29] Si $L_{2,3}$ spectra of SiO_x thin films with different stoichiometries have been previously reported by Baba et al.[30] Si K-edge
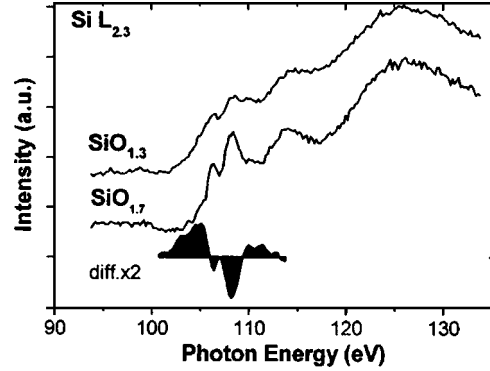

FIG. 5. Si $L_{2,3}$ absorption spectra of SiO_x thin films with different O/Si ratios. The shadowed curve corresponds to the difference spectra between the two plots.

absorption spectra of SiO_x samples exposed to the air have been also reported by several authors.[31] In a previous publication about the resonance behavior of the Auger peaks of $SiO_{1.3}$ thin films, we also discussed about the shape of the Si K-edge spectra,[10] although in that report, as in the present study, the samples were prepared and examined in situ. From the comparison of the different XAS results in literature for samples measured ex situ, it is evident that the correlation of the spectra with the O/Si ratio assumed for the films has to be done very cautiously because the samples, particularly at the most external layers, may undergo changes in stoichiometry by reaction with oxygen and water vapor of the atmosphere.

In the Si $L_{2,3}$ spectra in Fig. 5 for $SiO_{1.3}$ and $SiO_{1.7}$ samples, particularly in the spectrum of this latter, there are a series of well-defined peaks and broadened structures located at 106.2 (L_I), 108.3 (L_{II}), 114.1 (L_{III}), and $\sim$126.0 eV (L_{IV}). In a theoretical study by Chaboy et al.,[29] these authors attributed similar features found in SiO_2 to the t_2 representation of d-like orbitals (i.e., L_{IV} feature) and the e representation of the Si $3d$ levels hybridized with orbitals of the ligands (L_{III}). The difference between the spectra in Fig. 5 for samples $SiO_{1.7}$ and $SiO_{1.3}$ shows that the intensity of the two white line peaks decreases for the sample with the lowest oxygen content, while new available states develop at energies $E < 106.2$ eV. Some increase in intensity is also observed in this sample for an energy $E > 109$ eV, although the difference spectrum might not be completely accurate in this spectral region because of the large slope of the backgrounds of the two spectra in this figure. Baba et al.[30] have studied the Si $L_{2,3}$ spectra of SiO_x thin films produced by low-energy oxygen-ion implantation in Si(100) whose electronic structures are consistent with the MM. In those films the XAS spectra for x values higher than 0.4 were very similar to that of SiO_2 perhaps indicating that these SiO_x in situ samples have undergone oxidation by air exposure. The XAS spectra of Fig. 5 are completely different from those reported by Baba et al.[30] for the same O/Si ratios. This means that the conduction bands of the evaporated SiO_x films differ from that of SiO_2 (Ref. 30) even with stoichiometries as high as 1.7. In addition, the absorption feature at $E < 106.2$ eV can be attributed to the intermediate oxidation states present in our layers (see the XPS analysis of Fig. 1).
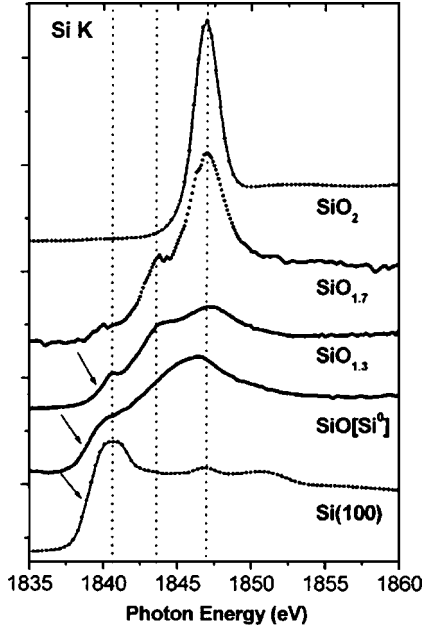
5

FIG. 6. Si K-edge absorption spectra of SiO$_x$ thin films of the indicated O/Si ratios. Sample SiO[Si^0] corresponds to a SiO$_{1.3}$ thin film heated at 750 K for 3 h under vacuum.

FIG. 7. (a) REELS spectra of sample SiO$_{1.7}$ recorded with increasing primary energies. (b) REELS spectra recorded with $E_0=2000$ eV for SiO$_x$ samples of different stoichiometries.

Figure 6 shows a series of K-edge absorption spectra for samples SiO$_{1.3}$ and SiO$_{1.7}$. For the sake of comparison, spectra of the Si(100), SiO$_2$, and Si[SiO$_2$] samples are also included in the figure. The latter sample corresponds to a SiO$_x$ thin film thermally activated in vacuum to produce the dismutation of the Si^{n+} ($n=1,3$) states into Si^0 and SiO$_2$ (Yubero SS-1999). The main feature for SiO$_2$ is a strong resonance at $\sim$1846 eV which decreases in intensity for samples with a lower content of oxygen. In the spectra of SiO$_x$ thin films the well-defined peaks at $\sim$1844 and $\sim$1841 eV grow in intensity with respect to the feature at $\sim$1846 eV as the oxygen content in the samples decreases. The spectrum of the SiO$_{1.3}$ thin film is similar to spectra previously reported by Flank et $al.$[32] and attributed by them to stoichiometric SiO. Meanwhile, the spectrum of Si^0 is characterized by a broad and low-intensity band at 1840 eV. The features at photon energies higher than 1842 eV in the Si(100) thin film are not present in polycrystalline silicon and will not be commented upon here.[31,33,34] These bands must not be confounded with the sharp peak situated at a slightly lower energy in the SiO$_x$ samples (i.e., at $\sim$1841 eV, cf. Fig. 6). This is clearly evidenced by comparison with the spectrum of the sample labeled as SiO[Si^0], where there is a mixture of Si^0 and SiO$_2$. Thus, the two sharp peaks at $\sim$1844 and $\sim$1841 eV present in the two SiO$_x$ samples have disappeared from the spectrum of SiO[Si^0], while the position of the absorption edge of this latter sample coincides with the edge position obtained for the Si^0 spectrum.

E. REELS spectra of SiO$_x$ thin films

Information about the distribution of the unoccupied states of a material can be also obtained by REELS. Figure 7 shows λK (normalized REELS) spectra for SiO$_x$ samples of dif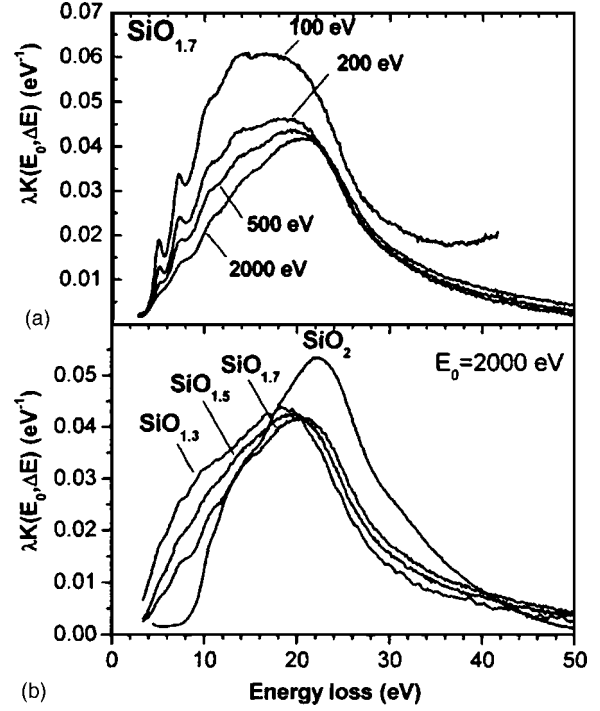ferent stoichiometries.[22,35] The shape of these spectra is the result of electronic transitions from the valence band to the conduction band plus the effect of collective excitations (plasmons) induced by the transport of a fast electron in the SiO$_x$ matrix. This figure also reports spectra of the SiO$_{1.7}$ sample recorded with various E_0 energies between 100 and 2000 eV. Spectra recorded with low primary energies are more surface sensitive because of the smaller information depth of these electrons.

Previous XPS characterization of the SiO$_{1.3}$ films reveals that they are mainly formed by Si^{3+} species.[10,12,18] This is corroborated by the features at 5.1 and 7.3 eV in the loss spectrum of SiO$_x$ that, in previous theoretical calculations, have been assigned to losses induced by neutral oxygen vacancies.[36] In our case these vacancies can be associated with silicon ions close to vacancies that very likely consists of Si^{3+} or Si$^+$ states. According to the spectra in Fig. 7 recorded with different electron energies for the SiO$_{1.7}$ thin film, these states should be majority at the topmost layers of the samples that, accordingly, would be heterogeneous in depth.

The energy of bulk plasmons is usually identified as the maximum of the main feature appearing in a loss spectrum. For the series of spectra in Fig. 7, the plasmon energy shifts to higher energies with the value of the O/Si ratio. The experimental relation between the bulk plasmon energy E_p and the value of x plotted in Fig. 8 can be described phenomenologically with the following expression obtained by linear regression of experimental points:
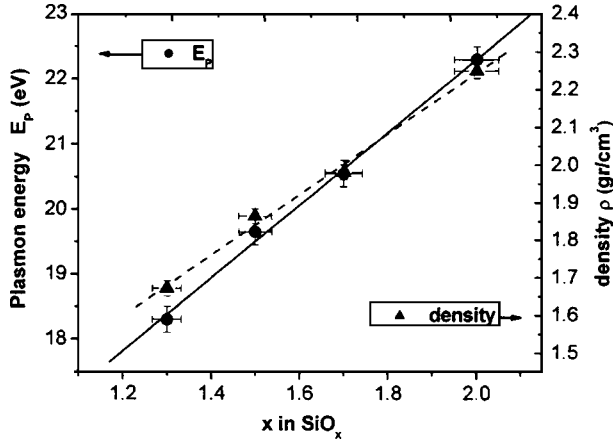
$$E_p = 22.36 - 5.62(2 - x). \tag{4}$$

FIG. 8. Position of the bulk plasmon and density of the films determined by means of expression (5) for samples with different O/Si ratios.

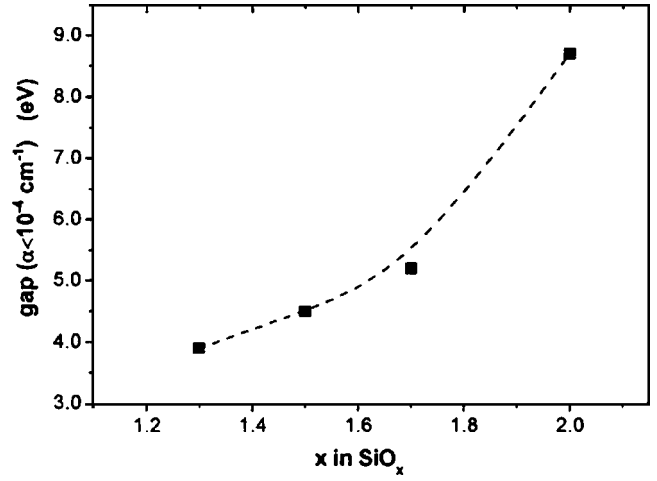

FIG. 9. Band-gap energies determined from the spectra in Fig. 7 ($E_0 = 2000$ eV) as a function of the content of oxygen in the films. The line has been plotted to guide the eyes.

The analysis of the REELS spectra provides a way to establish a relationship between the plasmon energy E_p and the density ρ of the material. In the free-electron approximation it holds that[19,37]

$$\rho = \frac{1}{829} \frac{ME_p^2}{N_v},\qquad(5)$$

where M is the molecular weight of the compound ($M = A_{Si} + xA_O$) and N_v is the density of the valence-band electrons ($N_v = N_{v_{Si}} + xN_{v_O}$). Thus, for SiO₂, with $E_p = 22.3$ eV, we obtain the expected bulk density value for silicon dioxide $\rho_{SiO_2} = 2.2$ g/cm³. Regarding the deposited SiO₁.₃, where $E_p = 18.6$ eV, we obtain $\rho_{SiO_{1.3}} = 1.7$ g/cm³. Note that the density of Si is 2.4 g/cm³. A lower density for SiO$_x$ ($x<2$) compounds than that of Si and SiO₂ have been previously reported by several authors.[1,13,19,38] From the series of samples analyzed in this study, the low density in the as-deposited SiO$_x$ films proves the formation of a new phase, and discards the possibility of considering the SiO$_x$ thin films prepared here as a mixture of segregated Si and SiO₂ domains.

For the series of thin films with variable O/Si ratios, the density is a linear function of the stoichiometry according to the following phenomenological expression derived by linear regression of the experimental points:

$$\rho(SiO_x) = 2.2 - 0.8(2 - x).\qquad(6)$$

This expression must be considered as derived from expression (4) relating plasmon energies with the stoichiometry of the films (i.e., refraction index and absorption coefficients).

It is apparent in Fig. 7 that the spectral intensity in the region of low-energy losses ($E<9$ eV) decreases until it nearly vanishes for SiO₂ where a clear band gap of ∼8 eV is observed. The evolution of band-gap energies estimated from the REELS spectra is plotted in Fig. 9 as a function of x. The reported values have been determined from the curves in Fig. 7 by linear fitting and extrapolation to zero intensity of the loss edges. It is interesting that while for the samples with $x < 1.7$ eV, the gap follows a linear relationship with x with a slope of ∼3.2-eV atomic ratio, it sharply increases for x

$= 2.0$ or values close to it. This result is in agreement with previous findings of Singh $et\ al.$[23] for SiO$_x$ thin films of different stoichiometries.

Optical properties in the UV region for energies higher than ∼4 eV can be obtained by the analysis of the REELS spectra. Details about this type of analysis have been given in Ref. 22 and the results are shown in Fig. 10. The determination of optical parameters for this energy region is not always straightforward and REELS may circumvent the use of synchrotron techniques, usually required for this purpose. It is apparent in this figure that in the range $4<E<20$ eV, the **n** function presents a decreasing tendency with the energy. In addition, the **n** curves shift to higher energies as x increases. It is interesting that the **n** curve for the SiO₂ thin film behaves differently and presents a well-defined maximum at ∼9.5 eV. For $E>20$ eV the n values are very similar for all the samples. Meanwhile, the **k** curves present a
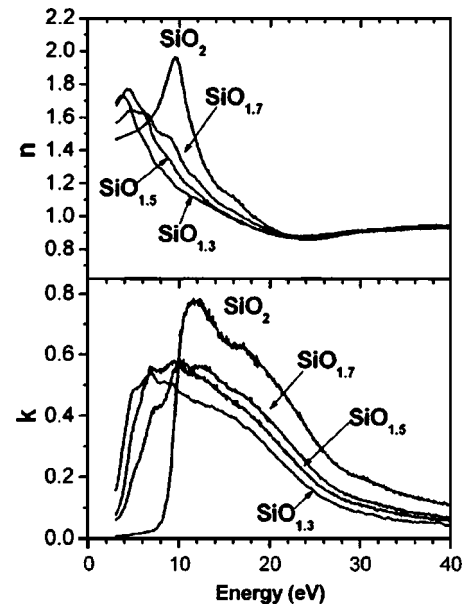

FIG. 10. **n** and **k** functions derived from the REELS spectra for the indicated SiO$_x$ samples.

maximum that shifts with composition from ~ 7 eV for $SiO_{1.3}$ to ~ 12 eV for SiO_2. This means that the SiO_x films become absorbent in the region with $E < 9$ eV, corresponding to the band gap of SiO_2. The formation of Si–Si bonds in the samples and the subsequent generation of associated electronic states must be responsible for this behavior. In fact, in samples with Si^{3+} and Si^+ species the absorption coefficient curve shows the appearance of electronic states in the region of the SiO_2 band gap. However, the fact that these states do not present any well-defined and intense loss feature produces that the refraction index does not present clear maxima in this region of the spectrum.

IV. CONCLUSIONS

The electronic properties of SiO_x thin films deposited at room temperature by evaporation from a silicon monoxide source have been characterized by a series of techniques including XPS, PES, Si K edge and $L_{2,3}$ XAS, and REELS. The films present a distribution of Si^{n+} states that differs from the predictions of the MM or RBM.

Several phenomenological expressions have been obtained that correlate the O/Si ratio of the films with their electronic, optical, or structural parameters determined by the different techniques. Empirical linear expressions have been derived for the Auger parameter values, the distance between some spectral features of the VB spectra, bulk plasmon energies, and film densities. It has been also shown that the energy distribution of occupied and unoccupied states is strongly dependent on the stoichiometry of the films. For the lowest stoichiometric thin films, the band gap amounted to ~ 3.8 eV while it increases smoothly up to a film composition of about $SiO_{1.7}$. Between $SiO_{1.7}$ and SiO_2 the band gap of the film increases sharply to about 8 eV.

For a O/Si ratio of 1.3, samples where Si^0 clusters have been prepared by thermal annealing depict a much lower energy gap which, in this case, is controlled by the low band-gap energy of elemental silicon. Samples with different O/Si ratios are characterized by a clear evolution of their electronic densities as determined by plasmon analysis. In parallel, it is shown that the value of the refraction index of these samples for $E > 4$ eV also increases. All these evidences indicate that in the absence of Si^0 clusters, the stoichiometry of these SiO_x materials can be considered as the main running parameter for the prediction of electronic and optical properties of the deposited materials. Also, it has been pointed out that the electronic properties of our films differ from those of other films with the same O/Si ratio reported in the literature (i.e., those whose distribution of Si^{n+} species is in agreement with the RBM or MM). In this regard, it must be concluded that not only the stoichiometry (i.e., O/Si ratio) but also the distribution of Si^{n+} species are key parameters for a straightforward comparison of the electronic structure of SiO_x thin films deposited by different techniques.

ACKNOWLEDGMENTS

[1] M. J. O'Leary and J. H. Thomas, III, J. Vac. Sci. Technol. A **5**, 106 (1987).
[2] *The Physics and Chemistry of SiO₂ and the Si−SiO₂ Interface*, edited by C. R. Helms and B. E. Deal (Plenum, New York, 1988).
[3] K. W. Wetcht, Appl. Opt. **30**, 4133 (1991).
[4] J. A. Savage, *Infrared Optical Materials and their Antireflection Coatings* (Adam Hilger, Ltd., Bristol, 1985).
[5] G. Hassand and C. D. Salzberg, J. Opt. Soc. Am. **44**, 181 (1954).
[6] L. Canham, Nature (London) **408**, 411 (2000).
[7] B. Gallas, C. C. Kao, S. Fisson, G. Vuye, J. Rivory, Y. Bernard, and C. Belouet, Appl. Surf. Sci. **185**, 317 (2002).
[8] F. Yun, B. J. Hinds, S. Hatatani, S. Oda, Q. X. Zhao, and M. Willander, Thin Solid Films **375**, 137 (2000).
[9] T. Shimizu-Iwayama, K. Fujita, S. Nakao, K. Sayito, T. Fujita, and N. Itoh, J. Appl. Phys. **75**, 7779 (1994).
[10] F. Yubero, A. Barranco, J. P. Espinós, and A. R. González-Elipe, Surf. Sci. **436**, 202 (1999).
[11] F. Rochet, G. Dufour, H. Roulet, B. Pelloie, J. Perrière, E. Fogarassy, A. Slaoui, and M. Fromment, Phys. Rev. B **37**, 6468 (1988).
[12] A. Barranco, J. A. Mejías, J. P. Espinós, A. Caballero, A. R. González-Elipe, and F. Yubero, J. Vac. Sci. Technol. A **19**, 136 (2001).
[13] F. G. Bell and L. Ley, Phys. Rev. B **37**, 8383 (1988).
[14] E. Martínez and F. Yndurain, Phys. Rev. B **24**, 5718 (1981).
[15] K. Hübner, A. Stern, and E. D. Klinkenberg, Phys. Status Solidi A **136**, 211 (1986).
[16] K. Haga and H. Watanabe, J. Non-Cryst. Solids **195**, 72 (1996).
[17] N. Tomozieu, E. E. van Faassen, W. M. Arnoldbik, A. M. Vredenberg, and F. H. P. M. Habraken, Thin Solid Films **420–421**, 382 (2002).
[18] A. Barranco, F. Yubero, J. P. Espinós, J. P. Holgado, A. Caballero, A. R. González-Elipe, and J. A. Mejías, Vacuum **67**, 491 (2002).
[19] J. P. Holgado, A. Barranco, F. Yubero, J. P. Espinós, and A. R. González-Elipe, Nucl. Instrum. Methods Phys. Res. B **187**, 465 (2002).
[20] A. Sassella *et al.*, J. Vac. Sci. Technol. A **15**, 377 (1997).
[21] P. G. Pai, S. S. Chao, Y. Takagi, and G. Lucovsky, J. Vac. Sci. Technol. A **4**, 689 (1986).
[22] F. Yubero, V. M. Jiménez, and A. R. González-Elipe, Surf. Sci. **400**, 116 (1998), and references therein.
[23] A. Singh, S. C. Bayliss, S. J. Gurman, and E. A. Davis, J. Non-Cryst. Solids **142**, 113 (1992).
[24] G. Zuther, Phys. Status Solidi A **59**, K109 (1980).
[25] A. R. Gonzalez-Elipe and F. Yubero, *Handbook of Surfaces and Interfaces of Materials*, edited by H. S. Nalwa (Academic, New York, 2001), p. 147, and references therein.
[26] R. Alfonsetti, L. Lozzi, M. Passacantando, P. Picozzi, and S. Santucci, Appl. Surf. Sci. **70/71**, 222 (1993).
[27] Y. Enta, Y. Miyanishi, H. Irimachi, N. Niwano, M. Suemitsu, N. Miyamoto, E. Shigemasa, and H. Kato, Phys. Rev. B **57**, 6294 (1998).
[28] J. Yeh and I. Lindau, At. Data Nucl. Data Tables **32**, 1 (1985).
[29] J. Chaboy, M. Benfatto, and I. Davoli, Phys. Rev. B **52**, 10014 (1995).
[30] Y. Baba, H. Yamamoto, and T. A. Sasaki, Phys. Rev. B **48**, 10972 (1993).
[31] C. Senemaud, M. T. Costa Lima, J. A. Roger, and A. Cachard, Chem. Phys. Lett. **26**, 431 (1974).
[32] A. M. Flank, R. C. Karnatak, C. Blancard, J. M. Esteva, P. Lagarde, and J. P. Connerade, Z. Phys. D: At., Mol. Clusters **21**, 357 (1991).
[33] N. Nagashima, A. Nakano, K. Ogata, M. Tamura, K. Sugawara, and K. Hayakawa, Phys. Rev. B **48**, 18257 (1993).
[34] T. Kashiwakura, H. Arai, N. Kozuka, K. Odagawa, T. Yokohama, A. Kamata, S. Nakai, J. Electron Spectrosc. Relat. Phenom. **79**, 207 (1996).
[35] S. Tougaard and I. Chokendorff, Phys. Rev. B **35**, 6570 (1987).
[36] F. Bart, M. Gautier, F. Jollet, and J. P. Duraud, Surf. Sci. **306**, 342 (1994).
[37] S. Tanuma, C. J. Powell, and D. R. Penn, Surf. Interface Anal. **17**, 927 (1991).
[38] S. M. A. Durrani, M. F. Al-Kuhaili, and E. E. Khawaja, J. Phys.: Condens. Matter **15**, 8123 (2003).